Macromolecular Research, Vol. 15, No. 1, pp 86-89 (2007)

Selective Poling and Characterization of Ferroelectric Poly(vinylidene fluoride-trifluoroethylene) by Scanning Nonlinear Dielectric Microscopy

Jong-Yoon Ha, Seok-Jin Yoon, and Dae-Yong Jeong*

Thin Film Research Center, Korea Institute of Sci. & Tech., Seoul 136-791, Korea

Yasuo Cho

Research Institute of Electrical Communication, Tohoku University, Japan

Received September 11, 2006; Revised November 20, 2006

Introduction

Domain engineering or patterning of ferroelectric materials is a very intriguing technique for the applications of high density memory, optical devices and nano-device applications.[1-9] Domain patterning has been applied to single crystals such as $LiTaO_3$ for high density storage memory applications. Domain patterns have been selectively mapped by pulsing an electric field through the nano-sized, conductive cantilever tip.[6-9] Thin single crystals with very flat surfaces are required, however, in order to reproduce nano-sized domain patterns precisely. These thin single crystals with extreme aspect ratios are difficult to fabricate.

One alternative to single crystals is the promising area of ferroelectric polymers. Ferroelectric polymers such as poly (vinylidene fluoride) and its copolymers, specifically poly-(vinylidine fluoride-trifluoroethylene) [P(VDF-TrFE)], have been the subject of intense study for over 25 years, yielding a wealth of physical data and practical applications.[10-15] In order for this polymer to exhibit desirable properties such as pyroelectricity and piezoelectricity, it must be poled to induce dipole alignment within the polymer crystals. To observe the resulting ferroelectric polarization, we apply the recently-developed technique of scanning nonlinear dielectric microscopy (SNDM), which is a novel electrical technique that permits imaging of the spatial ferroelectric polarization with sub-nanometer resolution.[6-8,16-20]

In this article, we investigate the polarization behavior of ferroelectric P(VDF-TrFE) polymer film that has been selectively poled with the technique of SNDM.

*Corresponding Authors. E-mail: dyjeong@kist.re.kr

Experimental

In order to create a polymer film, P(VDF-TrFE) copolymer with composition 83/17 mol% was dissolved in 1,4-dioxane. Platinum was sputtered on a glass substrate to serve as the bottom electrode. The polymer solution was then spin-coated. The films were then annealed at 130 °C for 3 hrs to increase the crystallinity. The film thickness used in this investigation was 400 nm.

We will briefly describe the basic principles of SNDM (a detailed description can be found elsewhere).[17-19] As shown in Figure 1, the SNDM instrument is primarily composed of the LC lumped constant resonator probe. In the figure, $C_s(t)$ denotes the capacitance between the central conductor (needle) and the outer conductor (the ring). This sample capacitance $C_s(t)$ is a function of time because the applied electric field $E_{P3}(=E_P\cos\omega_P t)$ is sinusoidal in time, and $C_s(t)$ can exhibit a nonlinear dielectric response. The ratio of the capacitance difference $\Delta C_s(t)$ to the static value of capacitance C_{s0} is

$$\frac{\Delta C_s(t)}{C_{S0}} = \frac{\varepsilon_{333}}{\varepsilon_{33}} E_P \cos\omega_P t + \frac{\varepsilon_{3333}}{4\varepsilon_{33}} E_P^2 \cos 2\omega_P t \qquad (1)$$

where ε_{33} is the linear dielectric constant and ε_{333} and ε_{3333} are nonlinear dielectric constants.

This LC resonator is connected to an oscillator tuned to the resonance frequency of the resonator. The oscillating frequency, about 1.3 GHz, is modulated by the change of capacitance $\Delta C_s(t)$ due to the nonlinear dielectric response. As a result, the oscillator produces a frequency modulated (FM) signal. By detecting this FM signal using the FM demodulator and lock-in amplifier, we obtain a voltage signal proportional to the capacitance variation. Each signal corresponding to ε_{333} and ε_{3333} was obtained by setting the reference signal of the lock-in amplifier at frequencies ω_p and $2\omega_p$ of

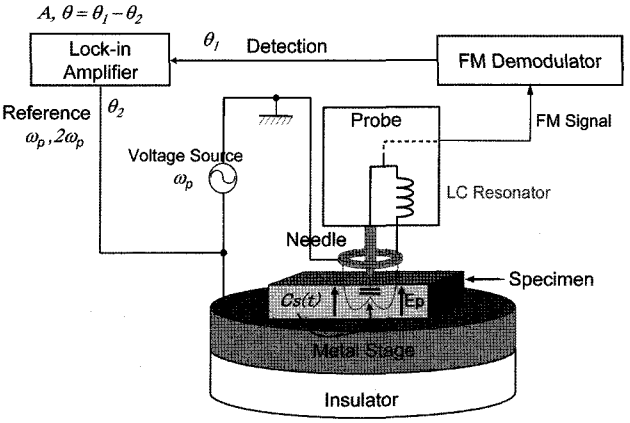

Figure 1. Schematic of the functional components of SNDM.

the applied electric field, respectively.

In this study, in order to apply the electric field and detect the electrical signal, we used as the probe a conductive AFM cantilever (Nanoworld, EFM-W). The cantilever was made of n-type Si coated with a PtIr metal film, and had a tip radius of 25 nm.

Generally, P(VDF-TrFE) copolymer has about 60 V/μm of coercive fields at room temperature.[21] First, selective poling was performed by applying dc voltage from 20 to 90 $V_{dc}/\mu m$ between the bottom electrode and the AFM cantilever tip while scanning an area of $2.0 \times 2.0\ \mu m^2$. To characterize the poling behavior, we performed simultaneous measurements of polarization and topography in an area of $10 \times 10\ \mu m^2$ that contained the poled area. In the experiments of SNDM imaging, the tip was held at electrical ground while a modulating voltage with a frequency of 8 kHz was applied to the bottom electrode.

Results and Discussion

Figure 2 shows the AFM and SNDM images for poling fields of 20, 45, and 90 $V_{dc}/\mu m$. For these SNDM images, $90V_{p\text{-}p}/\mu m$ modulating electric field was applied. While the AFM topographic image reveals no distinction within the polarized area, the SNDM images with the poling fields of 45 and 90 V/μm clearly reveal the positively-poled areas. As the dc field increases, P(VDF-TrFE) polymer was poled more strongly and the SNDM output signal increases.

At a poling field of 90 $V_{dc}/\mu m$, Figure 3 presents SNDM images for modulating fields of 20, 45, and 90 V/μm. The trend follows eq. (1): the SNDM signal intensity increases with modulating field amplitude. Alternately, Figure 4 presents the effect of polarization switching on the resulting image with a scan of negative poled area with positive dc bias. While the unpoled area results in a small positive

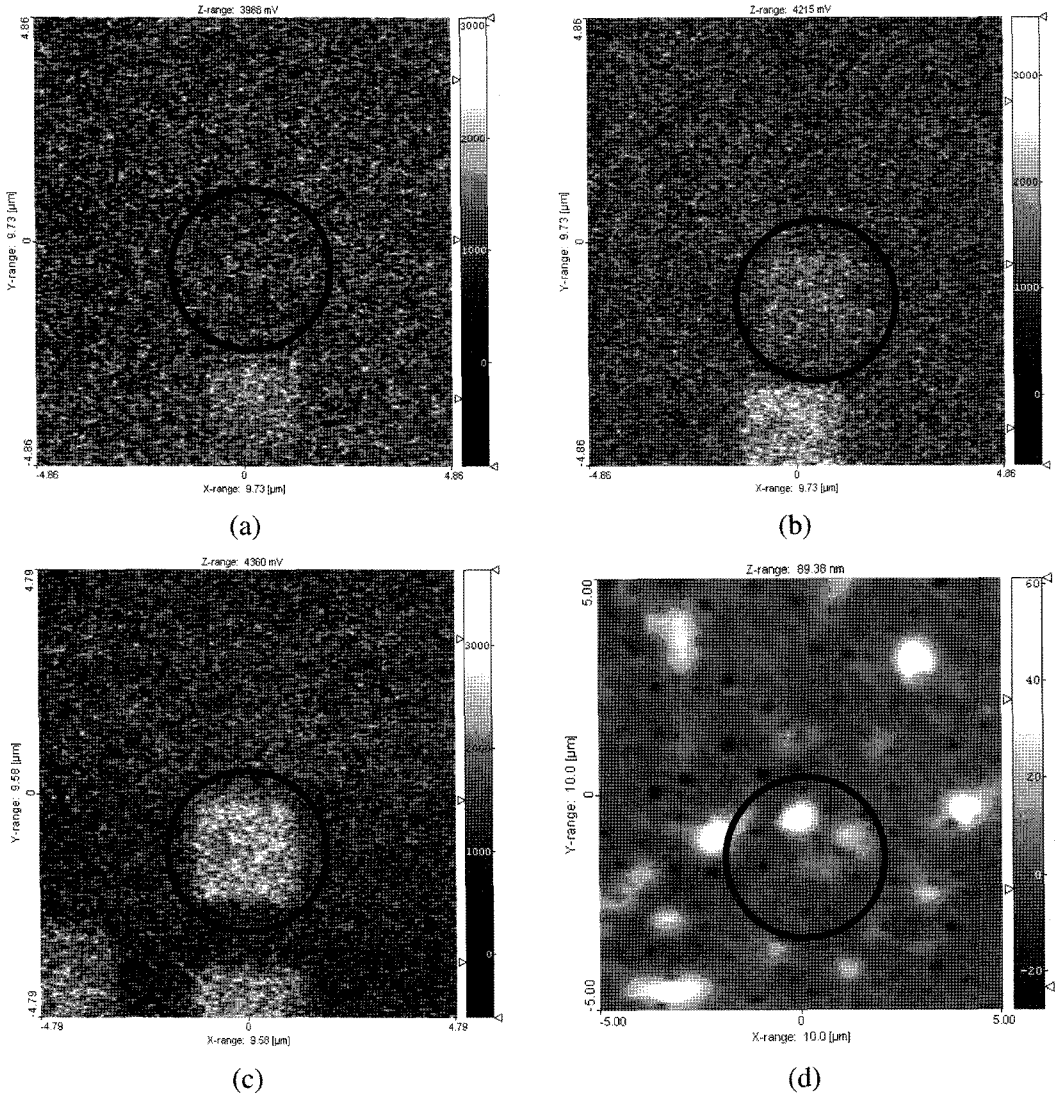

Figure 2. SNDM images with different poling field: (a) 20 $V_{dc}/\mu m$, (b) 45 $V_{dc}/\mu m$, and (c) 90 $V_{dc}/\mu m$. (d) AFM topograph.

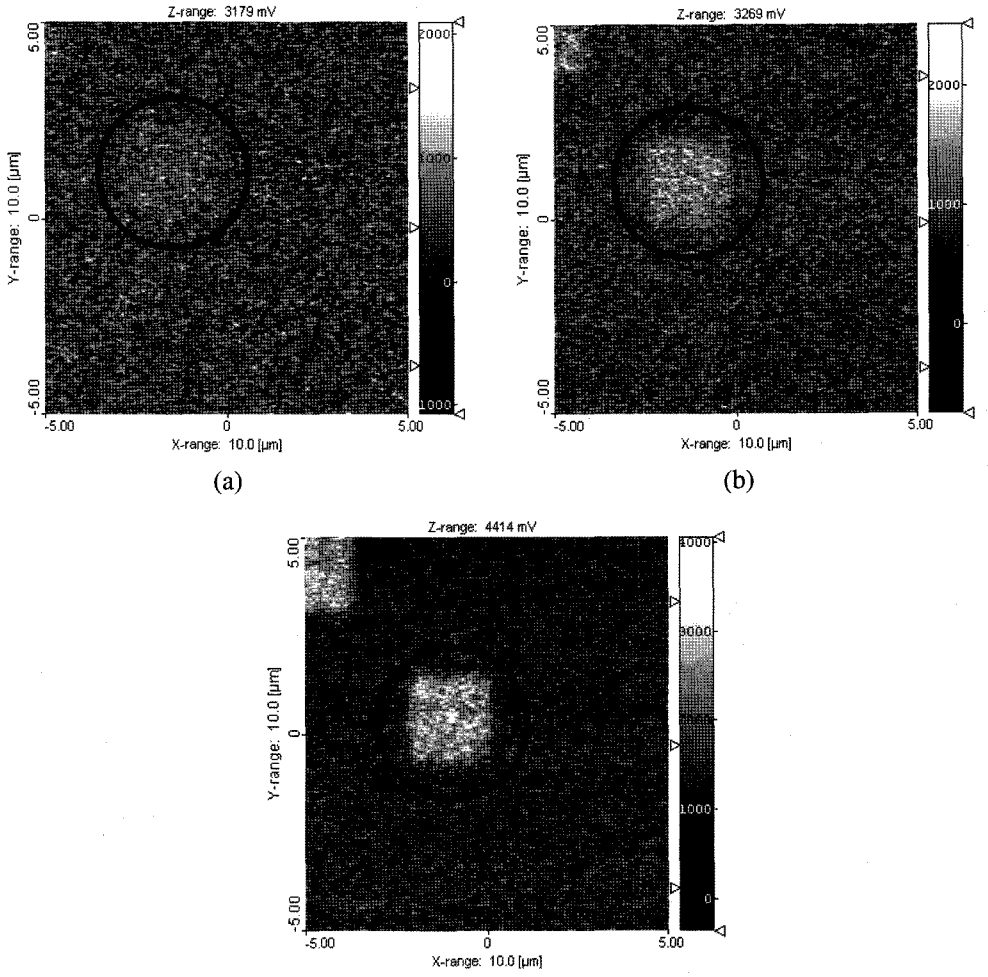

Figure 3. SNDM images with varying amplitude of the modulating field: (a) 20 $V_{p\text{-}p}/\mu m$, (b) 45 $V_{p\text{-}p}/\mu m$, and (c) 90 $V_{p\text{-}p}/\mu m$.

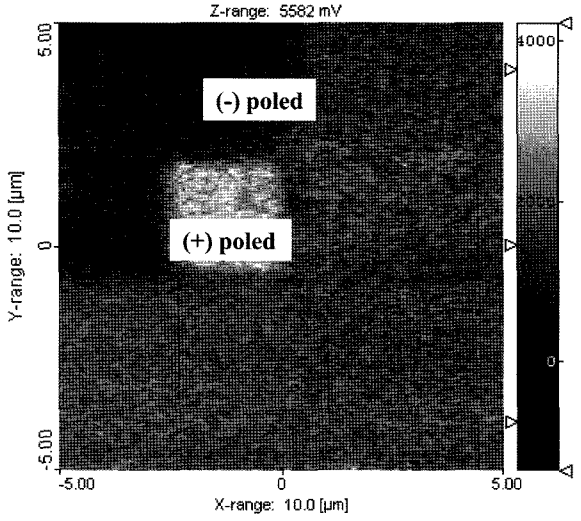

Figure 4. SNDM image with negatively and positively poled regions.

SNDM signal, the negatively poled area is dark (negative SNDM signal) and positive poled area shows bright (large positive SNDM signal) indicating that the dipole has been oriented to the electric field direction. The different appearance of the negatively poled region occurs due to the poling antiparallel to the detection field.

In theory, unpoled area should be centro-symmetric, giving SNDM signal should be zero. However, from the positive SNDM signal in unpoled area, it can be inferred that P(VDF-TrFE) polymer film might have the preferred orientation and further study is required to understand the origin of the preferred orientation.

Conclusions

We have successfully demonstrated a method to selectively pole small areas of thin P(VDF-TrFE) films with high precision, and then detect the degree and location of poling.

During the poling, stronger dc voltages resulted in the brighter regions apparent in the SNDM images, whereas negative dc voltages resulted in darker regions than the unpoled background. The concurrent topographical AFM images showed no change with poling. Finally, SNDM with the function of AFM has been shown to be a powerful tool for understanding the polarization behaviors of ferroelectric polymers.

References

(1) S. V. Kalinin, D. A. Bonnell, T. Alvarez, X. Lei, Z. Hu, R. Shao, and J. H. Ferris, *Adv. Mater.*, **16**, 795 (2004).
(2) X. Chen, H. Yamada, T. Horiuchi, and K. Matsushige, *Jpn. J. Appl. Phys.*, **38**, 3932 (1999).
(3) L. M. Blinov, R. Barberi, S. P. Palto, M. P. De Santo, and S. G. Yudin, *J. Appl. Phys.*, **89**, 3960 (2001).
(4) K. Kimura, K. Kobayashi, H. Yamada, T. Horiuchi, K. Ishida, and K. Matsushige, *Appl. Phys. Lett.*, **82**, 4050 (2003).
(5) S. Kim, V. Gopalan, K. Kitamura, and Y. Fukukawa, *J. Appl. Phys.*, **90**, 2949 (2001).
(6) K. Fujimoto and Y. Cho, *Appl. Phys. Lett.*, **83**, 5265 (2003).
(7) Y. Hiranaga and Y. Cho, *Jpn. J. Appl. Phys.*, **43**, 6632 (2004).
(8) Y. Hiranaga, Y. Cho, K. Fujimoto, Y. Wagatsuma, and A. Onoe, *Jpn. J. Appl. Phys.*, **42**, 6050 (2003).
(9) K. Fujimoto and Y. Cho, *Jpn. J. Appl. Phys.*, **43**, 2818 (2004).
(10) F. Xia, B. Razavi, H. Xu, Z.-Y. Cheng, and Q. M. Zhang, *J. Appl. Phys.*, **92**, 3111 (2002).
(11) F. Xia, H. Xu, F. Fang, B. Razavi, Z.-Y. Cheng, Y. Lu, B. Xu, and Q. M. Zhang, *Appl. Phys. Lett.*, **78**, 1122 (2001).
(12) B. Ploss and B. Ploss, *Polymer*, **41**, 6087 (2000).
(13) D.-Y. Jeong, *J. Kor. Phys. Soc.*, **44**, 1527 (2004).
(14) A. Bune, S. Ducharme, V. Fridkin, L. Blinov, S. Palto, N. Petukhova, and S. Yudin, *Appl. Phys. Lett.*, **67**, 3975 (1995).
(15) K. Tashiro and H. Hama, *Macromol. Res.*, **12**, 1 (2004).
(16) K. Ohara and Y. Cho, *Nanotechnology*, **16**, S54 (2005).
(17) T. Morita and Y. Cho, *Jpn. J. Appl. Phys.*, **42**, 6214 (2003).
(18) K. Ohara and Y. Cho, *Jpn. J. Appl. Phys.*, **41**, 4961 (2002).
(19) H. Odagawa and Y. Cho, *Surface Science*, **463**, L621 (2000).
(20) Y. Cho, A. Kirihara, and T. Saeki, *Rev. Sci. Instrum.*, **67**, 2297 (1996).
(21) Andrew J. Lovinger, *Science*, **220**, 1115 (1983).